

Isobaric Analog Resonances in Proton Scattering from ^{124}Te , ^{126}Te , ^{128}Te , and ^{130}Te †

J. L. FOSTER, JR.

The University of Texas, Austin, Texas 78712

and

The University of Pittsburgh, Pittsburgh, Pennsylvania 15213

AND

P. J. RILEY AND C. FRED MOORE

The University of Texas, Austin, Texas 78712

(Received 25 March 1968)

Isobaric analog states have been observed in proton elastic scattering from targets of ^{124}Te , ^{126}Te , ^{128}Te , and ^{130}Te . The levels thus observed in ^{125}I , ^{127}I , ^{129}I , and ^{131}I are analogs of low-lying levels of ^{126}Te , ^{127}Te , ^{129}Te , and ^{131}Te . Resonance parameters, Coulomb displacement energies, and spectroscopic factors have been extracted. Results are compared with (d,p) studies on the target nuclei.

I. INTRODUCTION

THE existence of analog states in light nuclei has been known for many years. As a result of experiments by Anderson *et al.*¹⁻⁴ and Fox *et al.*⁵⁻⁸ there has recently been a considerable renewal of interest in analog states, especially in heavy nuclei. Isobaric analog resonances have been shown to provide a useful and versatile tool for the study of nuclear structure. In this experiment, the observed resonances in the elastic scattering have been analyzed to obtain spectroscopic information and Coulomb displacement energies for the analog levels observed in ^{125}I , ^{127}I , ^{129}I , and ^{131}I . Comparisons have been made with the low-lying "parent" levels in ^{125}Te , ^{127}Te , ^{129}Te , and ^{131}Te which were previously reported and studied in (d,p) measurements on the even tellurium isotopes.⁹⁻¹¹

II. EXPERIMENT

The proton beam, collimated to a diameter of $\frac{3}{8}$ in., was obtained using the University of Texas EN tandem Van de Graaff accelerator. The beam energy was calibrated by using the $^{27}\text{Al}(p,n)$ threshold at 5.803 MeV: the absolute uncertainty in the calibration is about 25 keV. Targets consisted of separated

tellurium isotopes evaporated onto carbon backings. Target thicknesses, typically of the order of $50 \mu\text{g}/\text{cm}^2$ tellurium on $15 \mu\text{g}/\text{cm}^2$ carbon, were determined by elastic scattering measurements at 4-MeV proton energy. At this energy the cross section was assumed to arise from pure Rutherford scattering. Each datum point represents from 10^4 to 10^5 counts and the relative experimental errors are caused by target inhomogeneity and changes in solid angle as the beam wanders over the target. Absolute cross sections are believed to be good to 10%. Four solid-state detectors were used at laboratory angles of 90° , 120° , 150° , and 170° . The available detectors did not in general have sufficient depletion depth to stop the protons scattered from the target; thus, it was necessary to use uniform aluminum foils of thicknesses from 0.005 to 0.01 in. in front of the

† Work supported in part by the U.S. Atomic Energy Commission.

¹ J. D. Anderson and C. Wong, Phys. Rev. Letters **7**, 250 (1961).

² J. D. Anderson and C. Wong, Phys. Rev. Letters **8**, 442 (1962).

³ J. D. Anderson, C. Wong, and J. W. McClure, Phys. Rev. **126**, 2170 (1962).

⁴ J. D. Anderson, C. Wong, and J. W. McClure, Phys. Rev. **129**, 2718 (1963).

⁵ J. D. Fox, C. F. Moore, and D. Roson, Phys. Rev. Letters **12**, 198 (1964).

⁶ C. F. Moore, P. Richard, C. E. Watson, D. Robson, and J. D. Fox, Phys. Rev. **141**, 1166 (1966).

⁷ G. Yourvopoulos and J. D. Fox, Phys. Rev. **141**, 1180 (1966).

⁸ P. Richard, C. F. Moore, J. A. Becker, and J. D. Fox, Phys. Rev. **145**, 971 (1966).

⁹ R. K. Jolly, Phys. Rev. **136**, B683 (1964).

¹⁰ B. L. Cohen, C. L. Fink, and S. Hinds, Phys. Rev. **157**, 1144 (1967).

¹¹ A. Graue, E. Jastad, J. R. Lien, P. Torvund, and W. H. Moore, Nucl. Phys. **A103**, 209 (1967).

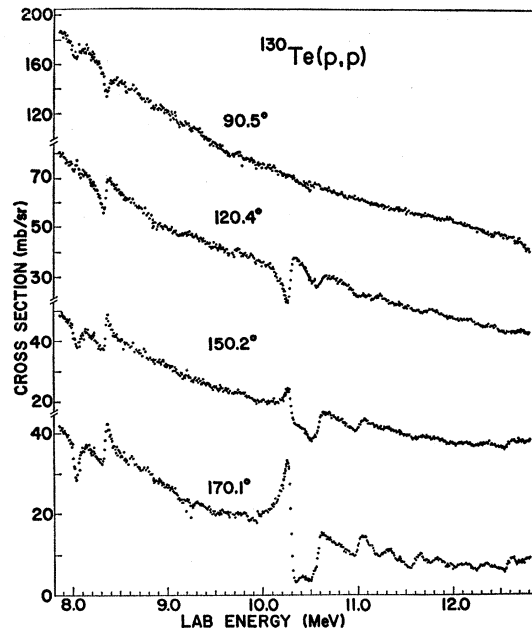
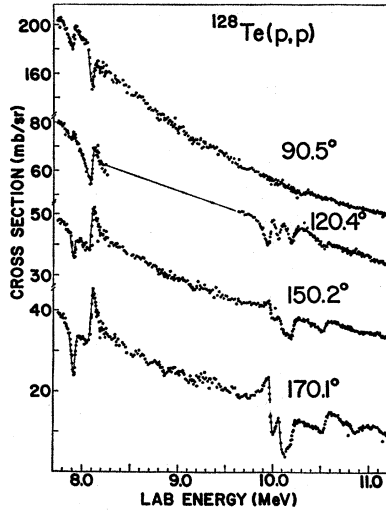


FIG. 1. ^{130}Te proton elastic scattering excitation functions.

FIG. 2. ^{128}Te proton elastic scattering excitation function.

detectors to degrade the incident proton energy. The elastic group resulting from scattering on tellurium was easily distinguishable from those of the carbon and oxygen impurities at these angles. Each counter was used in conjunction with one-quarter of a 400-channel analyzer. The spectra were transferred from the analyzer memory to an on-line PDP-7 computer and printed out on a line printer. A peak-summing program APHRODITE¹² summed the elastic peaks and printed out these sums together with the spectra. The data consist of excitation functions for elastic scattering for incident proton energies between approximately 7.5 and 11.5 MeV and are shown in Figs. 1-4. For ^{130}Te , the measurements were taken up to a proton energy of 12.7 MeV. In all cases the excitation functions were measured in approximately 8-keV intervals. Poor resolution as a result of the absorber foils and the limited number of analyzer channels available prevented observation of inelastic spectra, which when available should prove to be of interest.

III. ANALYSIS

A. Resonance Analysis

The elastic scattering cross sections at 90° , 120° , 150° , and 170° were fitted using code BRIGIT,^{13,14} which has been described elsewhere. The differential cross section for the elastic scattering of protons on spin-zero targets can be represented in terms of the scattering amplitude A and B in the following manner:

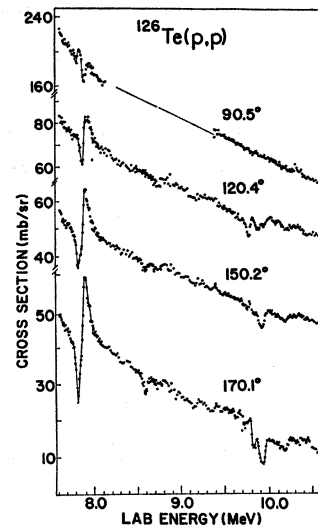
$$d\sigma/d\Omega = AA^* + BB^*. \quad (1)$$

By assuming that for the nonresonant scattering the spin-flip contribution is negligible it is possible to

¹² B. M. Foreman and C. F. Moore (unpublished).

¹³ C. F. Moore and L. Parish, Center for Nuclear Studies, University of Texas at Austin, Technical Report BRIGIT, 1967 (unpublished).

¹⁴ S. A. A. Zaidi, J. L. Parish, J. G. Kulleck, C. F. Moore, and P. von Brentano, Phys. Rev. 165, 1312 (1968).

FIG. 3. ^{126}Te proton elastic scattering excitation function.

express the amplitudes A and B as follows:

$$A' = e^{-i\gamma} A = \rho + \frac{1}{2k} \sum_{L,J} i(J + \frac{1}{2}) e^{i\alpha_L} \times \frac{i\Gamma_{L,J} P}{E_J - E - \frac{1}{2}i\Gamma_{L,J}} P_L^0(\cos\theta), \quad (2)$$

$$B' = e^{-i\gamma} B = -\frac{1}{2k} \sum_{L,J} (-1)^{L+J+1/2} e^{i\alpha_L} \times \frac{i\Gamma_{L,J} P}{E_J - E - \frac{1}{2}i\Gamma_{L,J}} P_L^1(\cos\theta),$$

where $\alpha_L = 2w_L + 2L - \gamma$.

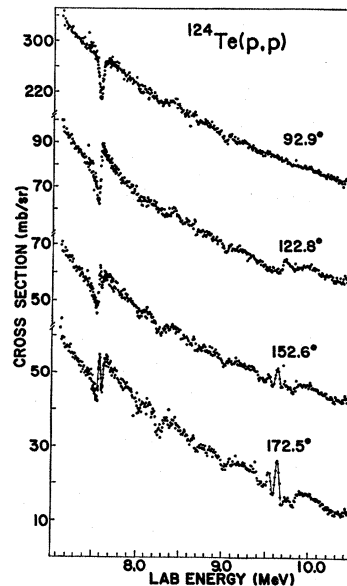
FIG. 4. ^{124}Te proton elastic scattering excitation function.

TABLE I. Comparison of results of $\text{Te}^{130}(p,p)$ and $\text{Te}^{130}(d,p)$ experiments. Quantities enclosed in parentheses are in some question.

(p,p)							(d,p)			
$E_{c.m.}$ (MeV)	$E_{c.m.}$ 7.977 (MeV)	Γ_p (keV)	Γ (keV)	l	J^π	S_{pp}	Excitation energy (MeV)	l_n	J^π	S_{dp}
7.977	0.00	8.5	77	2	$\frac{3}{2}^+$	0.26	0.00	2	$\frac{3}{2}^+$	0.25
							0.183	5	$1\frac{1}{2}$	0.17
8.282	0.305	10.2	60	0	$\frac{1}{2}^+$	0.10	0.297	0	$\frac{1}{2}^+$	0.16
							0.882	1	$(\frac{3}{2}^-)$	0.004
							1.043	0	$(\frac{1}{2}^+)$	0.005
(9.18)	1.21						1.209	2	$(\frac{5}{2}^+)$	0.02
(9.44)	1.47						1.471	1	$(\frac{3}{2}^-)$	0.005
							1.722	(1)	$(\frac{3}{2}^-)$	0.005
(9.75)	1.77						1.786	1	$(\frac{3}{2}^-)$	0.006
							2.014	1	$(\frac{3}{2}^-)$	0.002
							2.092	1	$(\frac{3}{2}^-)$	0.002
10.209	2.233	184	78	3	$\frac{7}{2}^-$	0.49	2.278	3	$\frac{7}{2}^-$	0.44
							2.329	(1)	$(\frac{3}{2}^-)$	0.004
							2.372	(1)	$(\frac{3}{2}^-)$	0.006
10.437	2.458	3.2	45	1	$\frac{3}{2}^-$	0.04	2.512	1	$(\frac{3}{2}^-)$	0.06
10.496	2.512	14.7	79	1	$\frac{3}{2}^-$	0.20	2.581	1	$(\frac{3}{2}^-)$	0.14
							2.752	1	$(\frac{3}{2}^-)$	0.005
10.895	2.918	18.9	103	1	$\frac{1}{2}$	0.20	2.002	1	$(\frac{3}{2}^-)$	0.19
11.007	3.030	(0.6)	(46)	(3)	$(\frac{5}{2}^-)$	(0.01)	3.141	(3)	$(\frac{5}{2}^-)$	0.004
11.07	3.10			3	$(\frac{5}{2}^-)$		3.183	(3)	$(\frac{5}{2}^-)$	0.005
11.46	3.49			(1)			3.353	3	$(\frac{3}{2}^-)$	0.003
11.59	3.62			(3)			3.663	2	$(\frac{5}{2}^+)$	0.03
11.66	3.69			(1)			3.686	1	$(\frac{3}{2}^-)$	0.05
							3.935	1	$(\frac{3}{2}^-)$	0.04
11.92	3.95			(1)			3.985	1	$(\frac{3}{2}^-)$	0.03
							4.028	1	$(\frac{3}{2}^-)$	0.07
							4.068	1	$(\frac{3}{2}^-)$	0.08
12.14	4.17			(1)			4.281	1	$(\frac{3}{2}^-)$	0.06
							4.297	(1)	$(\frac{3}{2}^-)$	0.05
12.23	4.26						4.323	1	$(\frac{3}{2}^-)$	0.03
							4.440	(1)	$(\frac{3}{2}^-)$	0.06
							4.487	(1)	$(\frac{3}{2}^-)$	0.05
12.48	4.50			(1)			4.543	(0)	$(\frac{3}{2}^+)$	0.08
							4.558	(0)	$(\frac{3}{2}^+)$	0.06
12.57	4.60						4.615	(2)	$(\frac{5}{2}^+)$	0.03
							4.644	(1)	$(\frac{3}{2}^-)$	0.05
12.75	4.78			(3)						

Code BRIGIT searches for the best values of the resonance parameters

$$E_J, \Gamma_{L,J}, \Gamma_{L,J^P}, \text{ and } \alpha_L.$$

The quantity $\rho(E)$, a slowly and monotonically changing function of energy, was simulated by a polynomial of fourth degree in inverse powers of E . In the fitting procedure, best-fit parameters were first obtained at one angle, usually 170° . The parameters were then varied to obtain the best over-all fit with the same resonance parameters at all four angles. This procedure allows unique resonance parameters to be obtained. The parameters are tabulated in Tables I-IV.

B. Spectroscopic Factors

A spectroscopic factor S_{pp} for an analog resonance may be defined for a spin-zero target by¹⁵

$$S_{pp} = \frac{(2T_0+1) \gamma_p^2(a_c)}{2J+1 \gamma_{sp}^2(a_c)}, \quad (3)$$

where γ_{sp}^2 = reduced width for a single-particle state, $T_0 = \frac{1}{2}(N-Z)$ = target isospin, and γ_p^2 = proton reduced width.

¹⁵ W. J. Thompson and J. L. Adams, Tandem Accelerator Laboratory, Florida State University, Technical Report ANSPEC, 1967 (unpublished).

TABLE II. Comparison of results of $\text{Te}^{128}(d,p)$ and $\text{Te}^{128}(p,p)$ experiments. Quantities enclosed in parentheses are in some question.

		(p,p)					(d,p)				
$E_{c.m.}$ (MeV)	$E_{c.m.}$ 7.854 (MeV)	l	J^π	Γ_p (keV)	Γ (keV)	S_{pp}	Excitation energy (MeV)	l_n	J^π	S_{dp}	
7.854	0.00	2	$\frac{3}{2}^+$	6.2	51	0.21	0.00	2	$\frac{3}{2}^+$	0.33	
							0.11	5	$\frac{1}{2}^-$	0.56	
8.048	0.194	0	$\frac{1}{2}^+$	9.9	48	0.09	0.17	0	$\frac{1}{2}^+$	0.37	
8.84	0.99						0.97	2	$(\frac{3}{2}^+)$	0.09	
9.17	1.32						1.28	2	$(\frac{3}{2}^+)$	0.01	
								4	$(\frac{7}{2}^+)$	0.07	
9.939	2.079	3	$\frac{7}{2}^-$	6.5	58	0.20	2.10	3	$(\frac{7}{2}^-)$	0.18	
10.049	2.195	3	$\frac{7}{2}^-$	4.7	56	0.14	2.22	3	$(\frac{7}{2}^-)$	0.25	
10.116	2.262	1	$(\frac{3}{2}^-)$	1.0	30	0.02					
10.172	2.318	1	$(\frac{3}{2}^-)$	13.0	103	0.20	2.36	3	$(\frac{3}{2}^-)$	0.31	
10.531	2.677	1	$(\frac{1}{2}^-)$	17	110	0.25	2.69	(1)	$(\frac{3}{2}^-)$	0.04	
								(5)	$(\frac{3}{2}^-)$	0.27	
(10.684)	(2.830)	(3)	$(\frac{5}{2}^-)$	(1.1)	(89)	(0.02)	2.83	1	$(\frac{3}{2}^-)$	0.32	
10.800	2.946	3	$(\frac{5}{2}^-)$	(1.4)	(62)	(0.03)	2.97	1	$(\frac{3}{2}^-)$	0.04	
(10.86)	(3.01)	(1)									
(11.09)	(3.24)	(3)					3.25	1	$(\frac{3}{2}^-)$	0.14	

Thompson *et al.*^{15,16} have devised a method to evaluate this expression. A bound-neutron wave function is used to determine γ_{sp}^2 by

$$\gamma_{sp}^2 = \frac{\hbar^2}{2M_n a_c} \frac{U_n^2(a_c)}{\int_0^{a_c} U_n(r) dr}, \quad (4)$$

where U_n is the radial neutron wave function for a single-particle state at the energy of the parent analog, M_n is the neutron mass, and a_c is the channel radius.

The R -matrix theory is reformulated in terms of optical-model wave functions in order to bypass the

nonresonant absorption problem in the evaluation of γ_p^2 . A result is

$$\gamma_p^2(a_c) = [\Gamma_p / 2P_{lJ}(a_c)] e^{2\delta_{lJ}}, \quad (5)$$

where Γ_p is the observed proton partial width, δ_{lJ} is the imaginary optical phase shift for a resonance of angular momentum l and spin J , and P_{lJ} is an optical-model penetrability. A computer program ANSPEC¹⁵ was used to evaluate these expressions and calculate spectroscopic factors.

Thompson has discussed the difficulties from a theoretical standpoint. From the point of view of the

TABLE III. Comparison of results of $\text{Te}^{124}(d,p)$ and $\text{Te}^{124}(p,p)$. Quantities enclosed in parentheses are in some question.

		(p,p)					(d,p)				
$E_{c.m.}$ (MeV)	$E_{c.m.}$ 7.482 (MeV)	Γ_p (keV)	Γ (keV)	l	J^π	S_{pp}	Excitation energy (MeV)	l_n	J^π	S_{dp}	
7.482	0.000	12.2	45	0	$\frac{1}{2}^+$	0.20	0.00	(0)	$\frac{1}{2}^+$	0.08	
7.515	0.033	4.8	38	2	$\frac{3}{2}^+$	0.24		(2)	$\frac{3}{2}^+$	0.24	
7.94	0.46			2							
8.15	0.67			2			0.64	2	$(\frac{5}{2}^+)$	0.04	
8.20	0.72			2			0.70	2	$(\frac{5}{2}^+)$	0.015	
8.29	0.81			2			0.77	(2)	$(\frac{3}{2}^+)$	0.006	
								(4)	$(\frac{7}{2}^+)$	0.04	
8.93	1.45										
9.30	1.82			3			1.81	2	$(\frac{3}{2}^+)$	0.014	
9.40	1.92			1			1.91	2	$(\frac{3}{2}^+)$	0.034	
9.47	1.99			3			1.98	(1)	$(\frac{3}{2}^-)$	0.009	
								(2)	$(\frac{3}{2}^+)$	0.011	
9.52	2.04			1			2.03	(1)	$(\frac{3}{2}^-)$	0.013	
								(2)	$(\frac{3}{2}^+)$	0.014	
9.58	2.10			3			2.11	(1)	$\frac{3}{2}^-$	0.05	
9.77	2.29			1							

¹⁶ W. J. Thompson, J. L. Adams, and D. Robson, Phys. Rev. **173**, 975 (1968).

TABLE IV. Results of $\text{Te}^{126}(p,p)$ and comparison with $\text{Te}^{126}(d,p)$. Quantities enclosed in parentheses are in some question.

$E_{c.m.}$ (MeV)	$E_{c.m.}$ 7.703 (MeV)	(p,p)			(d,p)					
		Γ_p (keV)	Γ (keV)	l	Excitation energy (MeV)	l_n	J^π	S_{dp}	S_{dp}	
7.703	0.00	5.65	43.2	2	0.00	2	$\frac{3}{2}^+$	0.22	0.49	
7.776	0.073	13.68	48.2	0	0.062	0	$\frac{1}{2}^+$	0.18	0.43	
					0.093	5	$\frac{11}{2}^-$		0.35	
					0.63	0			0.02	
8.483	0.792	1.60	52.32	2	0.79	2	$(\frac{5}{2}^+)$	0.02	0.09	
9.10					1.14	(2)	$(\frac{5}{2}^+)$		0.02	
					1.29	2	$(\frac{5}{2}^+)$		0.01	
9.10	1.40				1.40	0	$(\frac{1}{2}^+)$			
9.26	1.56				1.56	2	$(\frac{5}{2}^+)$		0.02	
9.54	1.84				1.82	1	$\frac{3}{2}^-$		0.006	
9.625	1.922	0.65	25.6	3	1.92	3	$\frac{7}{2}^-$	0.02	0.01	
9.692	1.989	1.60	44.7	1	2.00	1	$\frac{3}{2}^-$	0.03	0.03	
9.726	2.013	4.55	55.4	3	2.02	3	$\frac{7}{2}^-$	0.16	0.08	
					2.09	3	$\frac{7}{2}^-$		0.04	
9.809	2.106	4.24	64.0	3	2.13	3	$\frac{7}{2}^-$	0.14	0.09	
					2.16	3	$\frac{7}{2}^-$		0.01	
9.882	2.174	5.48	67.3	1	2.20	1	$\frac{3}{2}^-$	0.08	0.12	
					2.24	1	$\frac{3}{2}^-$		0.02	
10.00	2.30				2.32	3	$\frac{7}{2}^-$		0.05	
10.139	2.459	5.2	80.0	1	2.46	1	$\frac{3}{2}^-$	0.11	0.05	
					2.56	1	$\frac{3}{2}^-$		0.007	
					2.61	1	$\frac{3}{2}^-$		0.008	
					2.66	1	$\frac{3}{2}^-$		0.006	
10.30	2.69			(1)						
10.42	2.78			(3)						
					2.72	0	$\frac{1}{2}^+$		0.02	

calculation, there are two obvious problems:

(1) The proton states are unbound, while the neutron states are bound. Outside the nucleus, therefore, the single-particle parent-state function decays exponentially while the analog wave function must describe an outgoing wave. As a result, the calculated γ_{sp}^2 value is smaller than the correct value in the external region.

(2) The calculated penetrability, which is predominantly Coulomb, decreases with decreasing radii.

Thus, the product

$$S_{pp} = \frac{(2T_0+1) \Gamma_p e^{2\delta} i^j}{(2J+1) 2P_{1J}(a_c) \gamma_{sp}(a_c)^2} \quad (6)$$

should have a minimum for a channel radius near the nuclear radius. This minimum is observed in all cases and is taken as the value of the spectroscopic factor.

C. Optical Analysis

In order to provide an optical potential for the evaluation of spectroscopic factors, angular distributions were taken at off-resonance energies on ^{130}Te and ^{124}Te .

The optical-model potential used is shown below:

$$\begin{aligned}
 V(J,l,r) = & \left. \begin{aligned} & -V_s f(r, R_1, a_1) - iW f(r, R_2, a_2) \\ & -4a_3 iW' d f(r, R_3, a_3) / dr \end{aligned} \right\} \text{Central potential} \\
 & + \sigma \cdot 1 \left(\frac{\hbar^2}{m_\pi c} \right)^2 \frac{V_{so}}{r} \frac{d}{dr} f(r, R_4, a_4) \quad \text{Spin-orbit potential} \\
 & + \left. \begin{aligned} & (Ze^2/2R_c)(3-r^2/R_c^2), \text{ if } r \leq R_c \\ & + Ze^2/r, \text{ if } r > R_c. \end{aligned} \right\} \text{Coulomb potential}
 \end{aligned}$$

The function $f(r, R_i, a_i)$ is the usual Saxon-Wood shape:

$$f(r, R_i, a_i) = \{1 + \exp[(r - R_i)/a_i]\}^{-1}.$$

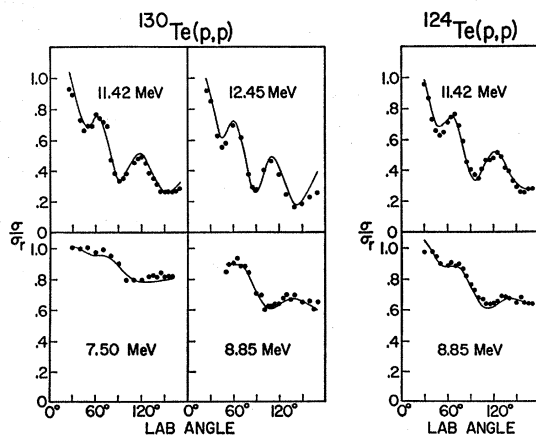


FIG. 5. (a) ^{130}Te optical-model fit of angular distributions. (b) ^{124}Te optical-model fits of angular distributions.

A computer program OPTIX¹⁷ has been written to solve the radial Schrödinger equation for the above (optical) potential.

The following optical parameters were found to produce good fits to the angular distributions: $R_1=R_2=R_3=R_0=1.22 A^{1/3}F$, $R_4=1.10 A^{1/3}F$, $a_1=a_2=a_3=a_4=0.650F$, $V=58.7$ MeV, $W=3.50$ MeV, $W'=6.00$ MeV, $V_{s0}=7.50$ MeV. Figures 5(a) and 5(b) show the optical fits for these parameters.

The values of R_1 , R_2 , R_3 , and R_4 were taken from the Coulomb displacement energy for a Saxon-Wood shape-charge distribution. The diffuseness parameters a_1 , a_2 , a_3 , and a_4 and the spin-orbit potential V_{s0} were given the average values of Perey. The final value of R_4 came from the polarization work of Veesper *et al.*¹⁸ on ¹³⁸Ba. The real potential well depth V , the volume absorption potential W , and the surface absorption potential W' were then obtained by fitting the angular distribution with the other parameters held fixed.

Excellent fits to the observed angular distributions have been obtained with optical parameters V , W , and W' which are very close to the average values of Perey.¹⁹ However, the $V_s R_1^2$ ambiguity makes the choice of R_1 somewhat arbitrary.

IV. RESULTS AND DISCUSSION

A. General Discussion

The individual resonances and the theoretical fits to them are shown in Figs. 6–12. The quality of the fits is generally good, giving corroboration to our interpretation of the excitation curves. Although the fits are extremely sensitive to the ratio Γ_p/T they are less sensitive to the total resonance width Γ . As a result, the proton partial widths Γ_p , and thus the spectroscopic factors, are believed to be about 20% uncertain even for the larger states. The relative resonance energies should be correct to within 10 keV while the systematic error due to the uncertainty in the analyzing magnet calibration is about 25 keV.

The orbital angular momentum of capture l for an isolated resonance is easily determined. A resonance appears as an anomaly in a potential scattering background, the anomaly being almost entirely due to interference between the resonant and background amplitudes. It can be seen from Eqs. (1) and (2) that the angular dependence of the interference is that of $P_l^0(\cos\theta)=P_l(\cos\theta)$. There is at most slight evidence of a resonance with angular momentum of capture l at the zeros of $P_l(\cos\theta)$ and there is a tendency for dips to become rises and for rises to become dips, on opposite sides of the zero.

¹⁷ W. J. Thompson and E. Gille, Tandem Accelerator Laboratory, Florida State University, Technical Report OPTIX 1, 1965 (unpublished).

¹⁸ L. Veesper, J. Ellis, and W. Haeberli, Phys. Rev. Letters **18**, 1063 (1967).

¹⁹ F. G. Perey, Phys. Rev. **131**, 745 (1963).

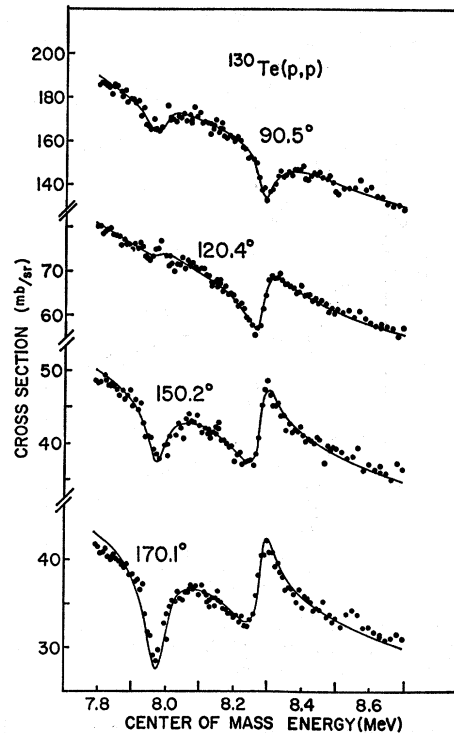


FIG. 6. ¹³⁰Te proton elastic scattering from 7.8 to 8.7 MeV. Center-of-mass angles are shown. The points are the data and the solid lines are the fits to the resonances at 7.977 and 8.282 MeV.

The total angular momentum J of a level cannot usually be ascertained directly from (d,p) measurements or proton elastic scattering differential cross sections. The level sequence and J values for the 82–126 neutron shell levels in the tellurium isotopes are very similar to

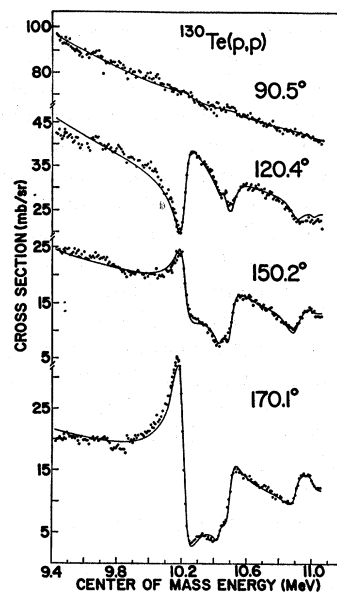


FIG. 7. ¹³⁰Te proton elastic scattering from 9.4 to 11.1 MeV. The points are the data and the solid lines are the fits to the resonances at 10.209, 10.437, 10.496, 10.895, and 11.007 MeV.

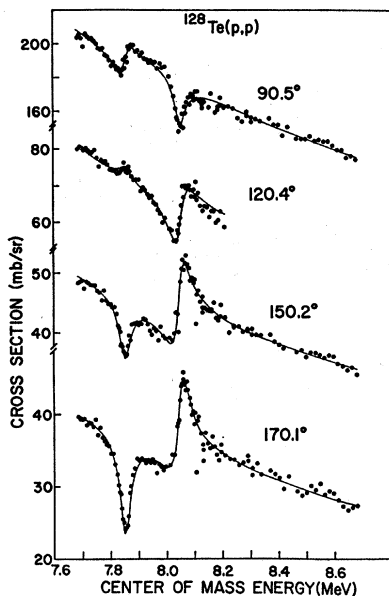


FIG. 8. ^{128}Te proton elastic scattering data from 7.7 to 8.7 MeV. The points are the data and the solid lines are the fits to the resonances at 7.854 and 8.048 MeV.

those of the $N=82$ isotopes on which several polarization measurements exist.^{18,20} For the 50–82 neutron shell, the spins which seemed to best correspond to the polarization measurements of Veaser *et al.*¹⁸ on ^{120}Sn were adopted, while for the 82–126 neutron shell, the spins which seemed most consistent with the 82-neutron nuclei polarization experiments are assumed.

B. Data and Individual Isotopes

^{131}Te - ^{131}I

Table I shows a comparison of parent analog states observed in ^{131}Te through the (d,p) reaction with the analog states observed in ^{131}I . The ^{131}Te states shown are the major levels seen by Graue *et al.* The low-lying analog states not observed in ^{131}I but seen in the (d,p) work have very small spectroscopic factors and involve proton energies below the Coulomb barrier, where low penetrabilities inhibit compound-nucleus formation. Orbital angular momenta assignments correspond well in the two measurements. At high excitation energies, neither set is completely reliable owing to numerous overlapping analog resonances and the very low beam energy (7.5 MeV) in Graue's (d,p) experiment. It was not possible in the elastic scattering work to make even a tentative assignment, with any confidence, for an l value greater than 3.

^{129}Te - ^{129}I and ^{125}Te - ^{125}I

Tables II and III show a comparison of the analog levels seen in ^{129}I and ^{125}I and the corresponding levels

in ^{129}Te and ^{125}Te seen by Jolly.⁹ The measurements of Jolly on the tellurium isotopes were made with a cyclotron having about 40-keV beam spread, and data were taken at only enough angles to determine the orbital angular momentum l_n associated with neutron capture. The small number of data points and the poor resolution caused a number of the l_n assignments in the (d,p) work to be in error. It has been possible in the present work to resolve and fit theoretically some proton analog resonances, the parent analogs of which could not be resolved in the (d,p) experiment.

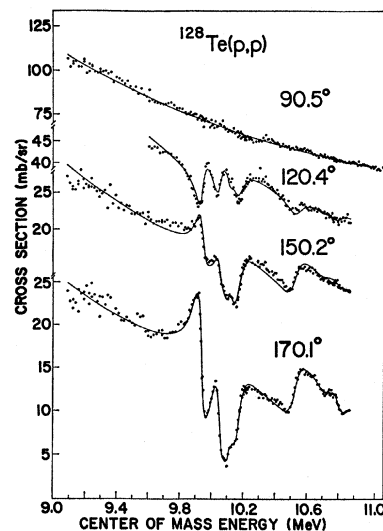


FIG. 9. ^{128}Te proton elastic scattering data from 9.1 to 10.9 MeV. The points are the data and the solid lines are the fits to the resonances at 9.939, 10.049, 10.116, 10.172, 10.531, 10.684, and 10.800 MeV.

For ^{129}Te and ^{129}I there is excellent agreement in l values and energy spacing for low-lying states. Above 2.25-MeV excitation there appear to be several additional small analog levels and there is some disagreement in l -value assignments.

For ^{125}Te and ^{125}I there is again excellent agreement in level positions. It was possible to resolve the ground and first excited analog states which could not be done in the (d,p) experiment. Figure 13 shows careful data taken between 9 and 10 MeV. A detector at 155° had sufficiently good resolution for the observation of the 0.606-MeV, 2^+ level in ^{124}Te by (p,p') . This peak is seen to resonate strongly on the analog states. Total lack of structure at 90° in the data between 9 and 10 MeV indicates there are no even l -value resonances in the region and that the identification of four states as $l_n=2$ in the (d,p) work was incorrect. Due to the very large number of resonances in the region between 9 and 10 MeV it would be quite difficult to obtain a unique set of resonance parameters. The region at 8.4-MeV excitation appears also to contain several overlapping resonances.

²⁰ G. Clausnitzer *et al.*, Nucl. Phys. A106, 99 (1968).

$^{127}\text{Te}-^{127}\text{I}$

Table IV shows a comparison of the analog states observed in ^{127}I and the levels seen in $^{127}\text{Te}(d,p)$ by Cohen *et al.*¹⁰ The (d,p) measurement, made with 16-keV resolution and at 12-MeV incident beam energy, allows an excellent comparison of the results of the analog experiment with the parent analog nucleus.

C. Spectroscopic Factor and the Shell Model

The method of extracting spectroscopic factors has been described in Sec. III B. Spectroscopic factors for the analog states are in good agreement with the (d,p) work except for the $\frac{1}{2}^+$ resonances which have uniformly lower spectroscopic factors. Minimum S_{pp} values occurred at radii of $6.1 \pm 0.2 \text{ F}$ for $3s_{1/2}$, $2d_{3/2}$, and $2d_{5/2}$ resonances and at radii of $7.0 \pm 0.2 \text{ F}$ for $2f_{7/2}$, $3p_{3/2}$, $3p_{1/2}$, and $2f_{5/2}$ resonances (82-neutron shell).

Table V shows the sums of the spectroscopic factors and the single-quasiparticle energies for the states

The number n of neutrons in subshell with spin j is given by

$$(2j+1)V_j^2 = nj.$$

One expects that

$$\sum_m S_j^m \simeq U_j^2.$$

The $h_{11/2}$ spectroscopic factors were obtained by determining the number of holes in the $d_{5/2}$, $g_{7/2}$, $s_{1/2}$, and $d_{3/2}$ subshells, then subtracting this from the total number of holes expected in the 50 to 82 neutron shell assuming negligible filling of the next shell. Single-quasiparticle energies \bar{E}_j were determined by taking a weighted average of excitation energy over all the observed members of a single-particle transition multiplet as

$$E_j = \frac{\sum_m S_j^m E_j^m}{\sum_m S_j^m}.$$

Energies for the $d_{5/2}$, $g_{7/2}$, and $h_{11/2}$ multiplets were obtained from the (d,p) experiments.

Pairing theory²¹ gives the relation

$$U_j^2 = \frac{1}{2} \{ 1 + (\epsilon_j - \lambda) / [(\epsilon_j - \lambda)^2 + \Delta^2]^{1/2} \},$$

where the ϵ_j are single-particle energies of the shell model, λ is the Fermi energy, and Δ is half of the "energy gap". Table VI shows that U_j^2 for the $d_{3/2}$, $s_{1/2}$, and $h_{11/2}$ single-quasiparticle states predicted by pairing theory, using the parameters of Kisslinger and Sorensen²¹ for the Te isotopes and isotonic Xe isotopes when parameters are not available for tellurium.

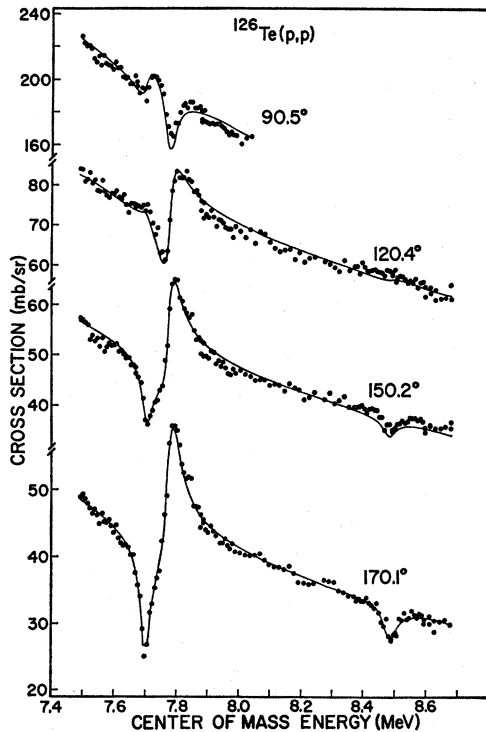


FIG. 10. ^{126}Te proton elastic scattering data from 7.5 to 8.7 MeV. The points are the data and the solid lines are the fits to the resonances at 7.703, 7.776, and 8.483 MeV.

observed in the odd tellurium isotopes in the analog-state experiments. The $d_{5/2}$ and $g_{7/2}$ spectroscopic factors were obtained from the (d,p) experiments. The "emptiness" of a subshell U_j^2 and the "fullness" V_j^2 satisfy the equation

$$U_j^2 + V_j^2 = 1.$$

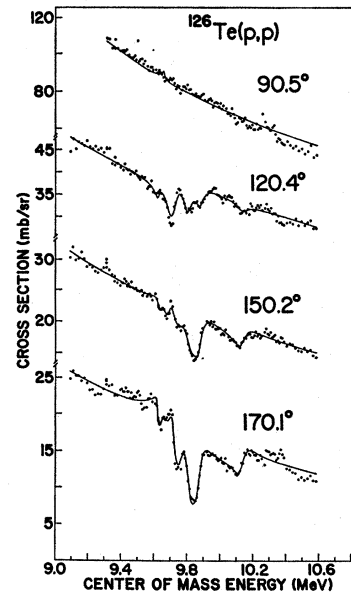


FIG. 11. ^{126}Te proton elastic scattering data from 9.1 to 10.6 MeV. The points are the data and the solid lines are the fits to the resonances at 9.625, 9.692, 9.726, 9.809, 9.882, and 10.139 MeV.

²¹L. S. Kisslinger and R. A. Sorensen, *Rev. Mod. Phys.* **35**, 853 (1963).

TABLE V. The sums of the spectroscopic factors $\sum_m S_j^m$ and the average energies \bar{E}_j for the observed analog levels of the single-quasiparticle states in the odd tellurium isotopes.

State	Te^{121}		Te^{123}		Te^{127}		Te^{125}	
	$\sum_m S_j^m$	\bar{E}_j						
$d_{3/2}$	0.26	0.0	0.21	0.0	0.22	0.0	0.24	0.03
$s_{1/2}$	0.10	0.30	0.09	0.17	0.18	0.07	0.20	0.0
$h_{11/2}$	(0.22)	(0.18)	(0.32)	(0.11)	(0.50)	(0.09)	(0.66)	(0.15)
$g_{7/2}$			(0.07)	(1.01)	(0.14)	(1.27)	(0.11)	(0.65)
$f_{7/2}$	0.49	2.28	0.34	2.13	0.32	2.05		
$p_{3/2}$	0.24	2.50	0.22	2.31	0.11	2.12		
$p_{1/2}$	0.20	3.00	0.25	2.68	0.11	2.46		
$f_{5/2}$			0.05	2.90				

D. Coulomb Displacement Energies

The Coulomb displacement energy ΔE_c between the analog and the parent analog state is given by the relationship

$$\Delta E_c = E_p + \Delta_{dp} + 2.225 \text{ MeV},$$

where E_p is the center-of-mass proton energy at which the analog resonance in the nucleus $(N, Z+1)$ occurs, Q_{dp} is the (d, p) reaction Q value, and 2.225 MeV is the deuteron binding energy. The results are shown in Table VII and are compared with ΔE_c values computed using the empirical relation of Long *et al.*²²:

$$\Delta E_c = B_1 + B_2 Z(A)^{-1/3},$$

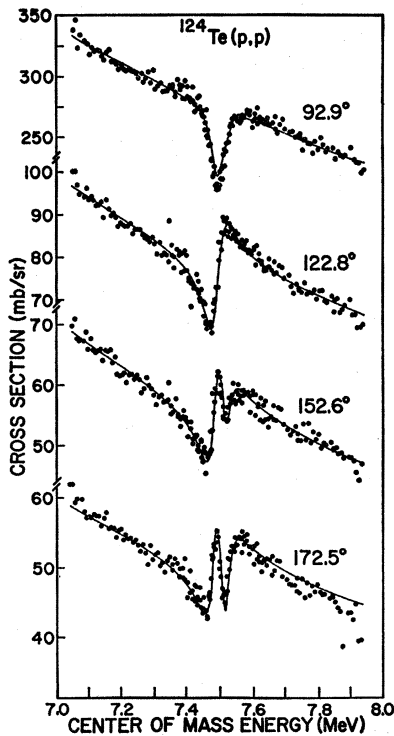


FIG. 12. ^{124}Te proton elastic scattering data from 7.0 to 7.9 MeV. The points are the data and the solid lines are the fits to the resonances at 7.482 and 7.515 MeV.

²² D. D. Long, P. Richard, C. F. Moore, and J. D. Fox, Phys. Rev. 149, 906 (1966).

where $B_1 = -1.032$ and $B_2 = 1.448$. Z and A are the charge and mass numbers for the parent analog nucleus. The measured Coulomb displacement energies agree with those predicted by the relation of Long *et al.* to well within the analyzing-magnet calibration error.

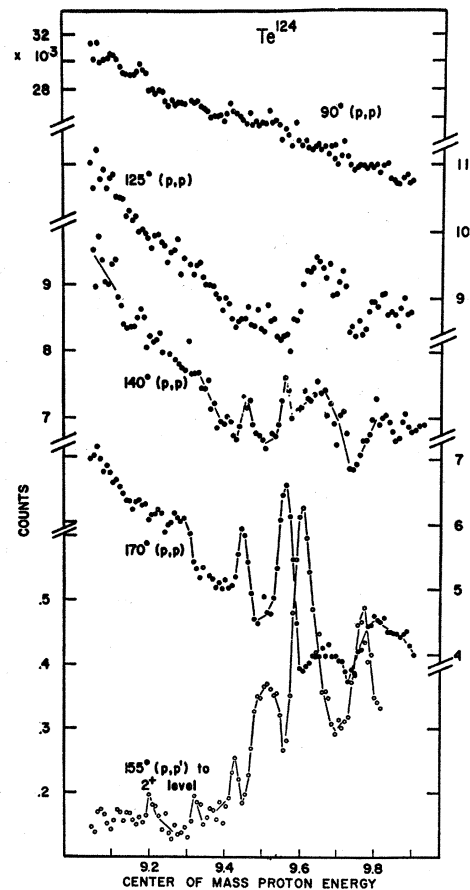


FIG. 13. ^{124}Te proton scattering data from 9.0 to 10.0 MeV. Counts appear as a function of center-of-mass proton energy. Laboratory angles are shown. The solid points are elastic scattering data and the hollow circles are inelastic scattering data to the 2^+ , 0.606-MeV level of ^{124}Te . There appear to be the following resonances: 9.30 MeV, f wave; 9.40 MeV, p wave; 9.47 MeV, f wave; 9.52 MeV, p wave; 9.58 MeV, f wave and 10.77 MeV, p wave.

TABLE VI. Comparison of experimental and theoretical values of U_j^2 .

	Te^{181}		Te^{129}		Te^{127}		Te^{126}	
	Theory	Expt	Theory	Expt	Theory	Expt	Theory	Expt
$d_{3/2}$	0.25	0.26	0.37	0.21	0.47	0.22	0.57	0.24
$s_{1/2}$	0.03	0.10	0.06	0.09	0.09	0.18	0.18	0.20
$h_{11/2}$	0.16	0.22	0.26	0.32	0.37	0.50	0.47	0.66

V. SUMMARY

The correspondence between the proton analog states in the tellurium isotopes and the parent states in (d, p) measurements from the same targets is in agreement with the existence of a proton analog state in the nucleus ($N, Z+1$) for every level in the ($N+1, Z$) nucleus. The analysis of the elastic scattering data has been shown to supplement the (d, p) analysis, and in some cases has yielded new spectroscopic information. The ground state of ^{181}Te , with three holes in a closed shell of 82 neutrons, has the simplest level structure of the odd- A tellurium isotopes investigated. The complexity of the

TABLE VII. Results (see text).

Target isotope	Analog pair	Q_{dp} (MeV)	E_p (MeV)	ΔE_c (MeV) (Measured)	ΔE_c (MeV) (Long <i>et al.</i>)
^{124}Te	$^{128}Te-^{126}I$	4.33	7.497	14.052	14.027
^{126}Te	$^{127}Te-^{127}I$	4.00	7.704	13.928	13.946
^{128}Te	$^{129}Te-^{129}I$	3.79	7.846	13.862	13.870
^{130}Te	$^{131}Te-^{131}I$	3.61	7.962	13.801	13.795

level scheme increases as one moves further from the closed neutron shell. The high density of states and the smaller cross sections for individual transitions makes the analysis of the high excitation $^{124}Te(p, p)$ data nearly impossible.

ACKNOWLEDGMENTS

The authors wish to express their appreciation to Dr. B. B. Kinsey for his interest in and support of the experiment. Thanks are also due to C. G. Shugart and G. A. Lock for assistance in taking the data, and to E. Riley for the preparation of the drawings.

Decay Studies of Iodine-118 and -120*

INGE-MARIA LADENBAUER-BELLIS AND H. BAKHRU

Yale University, New Haven, Connecticut 06520

(Received 15 May 1968)

The radioactive decay of iodine-118 ground and isomeric state and iodine-120 ground and isomeric state from irradiations of silver with carbon-12 ions, palladium with nitrogen-14 ions, and cadmium with boron-11 ions has been studied with a germanium lithium-drifted detector, a NaI crystal, an anthracene crystal, and several 400-channel analyzers. The electron and γ spectra, and singles and coincidence spectra, have been interpreted. Tentative decay schemes for the iodine-118 ground state and isomeric state as well as the iodine-120 ground state and isomeric state are given. The half-life of I^{118g} was found to be 13.0 ± 0.3 min (γ -ray energies: 542, 605, and 1147 keV, β^+ endpoint energy: 6.05 MeV). The half-life of the isomeric state was found to be 8.5 ± 0.5 min (γ -ray energies: 600 and 612 keV). The half-life of I^{120g} was found to be 83 ± 4 min (γ -ray energies: 560, 640, 1520, and 1540 keV, β^+ endpoint energies: 3.45 and 2.9 MeV). The half-life of the isomeric state was found to be 53 ± 4 min (γ -ray energies: 600 and 612 keV, β^+ endpoint energy: 3.85 MeV). A comparison of the levels of $Te^{118, 120, 122, 124, 126}$ is given.

1. INTRODUCTION

THE neutron-deficient isotopes of iodine were first investigated in connection with the spallation reaction of lanthanum and the fission reaction of uranium with 19-GeV protons by Andersson *et al.*¹ After an electromagnetic isotope separation iodine-118 was found to have a half-life of (13.9 ± 0.5) min and γ rays of 511, 555, 605 and 1150 keV. The half-life of iodine-120 was determined to be 1.35 ± 0.01 h and the corresponding γ rays measured with a NaI(Tl) detector

system were found to have the following energies: 511, 560, 620, (1190), and 1520 keV.

When this work was initiated, no high-resolution experiments had been performed on these neutron-deficient isotopes. Furthermore, the decay characteristics of these isotopes were not known. The present study with the high-resolution Ge(Li) detectors was undertaken to obtain more information on these isotopes with better energy determination of the close-lying γ rays. Also the availability of heavy-ion beams from the Yale Heavy-Ion Accelerator made it possible to produce these isotopes in relatively clean form. The decay properties of I^{118} and I^{120} will be discussed in this paper.

* Work supported by the U. S. Atomic Energy Commission.

¹ G. Andersson, G. Rudstam, and G. Sorensen, *Arkiv Fysik* 28, 37 (1965).